Chemical Engineering Journal 113 (2005) 187–196

Chemical Engineering Journal

www.elsevier.com/locate/cej

Review

A phenomenological review of biofilter models

Joseph S. Devinny *, J. Ramesh

Civil and Environmental Engineering, University of Southern California, Los Angeles, CA 90089-2531, USA

Received 13 December 2004; received in revised form 27 February 2005; accepted 3 March 2005

Abstract

Many mathematical models have been created in an effort to improve our understanding of biofilters, to guide experimentation, and to improve design of biological treatment systems. The approaches used to model gas flow, phase transfer, diffusion within the biofilm, and biological growth have become relatively standard. Further progress on these phenomena will come primarily from improved determinations of important model parameters under various conditions. There is less unanimity and less certainty in the approaches that have been taken to account for biofilm growth, the complex conformation of the biofilm takes within the porous packing, and the details of the processes by which biofilters become clogged. Biofilter and biotrickling filter models have been useful for research purposes, but have not yet progressed to the point of being reliable and generally accepted tools for design.

Keywords: Biofilter; Biofiltration; Biotrickling filter; Models

1. Introduction

Many investigators have created mathematical models of biofilters and biotrickling filters in their efforts to understand and improve reactor performance. While there has been significant success among investigators in describing and understanding laboratory results, no single model has become a generally accepted standard. Each research group has developed its own approach, often specific to the experiments being performed. Design of full-scale applications is still largely done by rule of thumb, and application of biofilters to effluents under previously untested conditions of concentration, concentration fluctuation, and contaminant mix often requires pilot-scale testing.

This work reviews many of the existing models in an effort to define the range of efforts and to identify trends in the approaches. Results were organized in terms of the phenomena studied, rather than by investigators. Notation varies widely in the literature, and has been converted here to a single convention. Because the equations are primarily used for description, the notation has been made as explanatory as possible rather than brief. Some of the equations, such as those describing advection in the gas phase, are generally accepted and widely used in models, so no effort has been made to ascribe them to individual investigators.

Biological air treatment may use either biofilters or biotrickling filters. By definition, biofilters are kept wet, but there is no moving water phase, while water is constantly applied to biotrickling filters, producing a film of water that flows over the packing and the biofilm. In practice, however, biofilters are often washed with water at intervals to ensure adequate biofilm water content. Some are washed for as much as 20 min in each hour. On the other hand, water flow is inevitably interrupted from time to time in biotrickling filters, and it is recognized that because unsaturated gravitational flow in porous media is so irregular, biotrickling filters are likely to include considerable volumes that are not being washed. Thus, biological systems range from true biofilters at one extreme to true biotrickling filters at the other, and most systems lie somewhere between. Many of the phenomena modeled apply equally to biofilters and biotrickling filters. Others, however, may be specific to one type.

The purpose of this paper is to describe the efforts that have been made to create mathematical descriptions of biofilters and biotrickling filter. Review on a model-by-model or

* Corresponding author. Tel.: +1 213 740 0670.
E-mail address: devinny@usc.edu (J.S. Devinny).

1385-8947/$ – see front matter © 2005 Elsevier B.V. All rights reserved.
doi:10.1016/j.cej.2005.03.005

Nomenclature

a	fitted constant in equation for maximum evaporation rate
a_0, a_{bf}	specific surface area of packing, biofilm
A	inverse width constant for description of pH effects
b	death rate constant for biomass
B	pH of maximum biodegradation rate
c	fitted constant in equation for maximum evaporation rate
C_{ads}, C_{adseq}, C_{air}, C_{bf}, C_{ibf}, C_{jbf}, C_{bfbot}	concentration of contaminant adsorbed on the medium, adsorbed on the medium at equilibrium, in the air, in the biofilm, species i in the biofilm, species j in the biofilm, and in the biofilm at the bottom
C_{Nbf}, C_{O_2bf}, C_{Rbf}	concentrations in the biofilm; of nutrient, oxygen, and reactant
d	fitted constant in equation for maximum evaporation rate
D_{air}, D_{bf}, D_w	diffusion coefficient for contaminant; in air, biofilm, water
D_{flow}	dispersion coefficient for air flowing through reactor
D_R	diffusion constant for reactant nutrient in biofilm
EC_{max}	maximum reactor elimination capacity
F_{pH}	biodegradation rate multiplier for effects of pH
g	acceleration of gravity
H	Henry's Law constant
H_T	height of biotrickling filter
ΔH	heat of adsorption, contaminant on packing
J_{bf}, J_{ads}	flux of contaminant per unit area into the biofilm from the air, to adsorption on the packing from the biofilm
$k_{air–bf}$	contaminant transfer rate coefficient, air to biofilm
K_0	equilibrium constant for Arrhenius adsorption on solid
K_{ads}	linear adsorption constant for contaminant on the packing
K_{inh}	Haldane constant for inhibition between species i and j
K_S, K_{SR}, K_{SO_2}, K_{Si}, K_d	Monod half-saturation rate constants for contaminant, nutrients, oxygen, contaminant i, and biomass death
L_{bf}	thickness of the biofilm
M_C, M_R	molecular weight of contaminant, reactant
n	average number of contacts between spherical packing particles
p_{ij}	constants for inhibition of degradation of contaminant i by contaminant j
Q_w	biotrickling filter water flow rate
R	gas constant
Re	Reynolds number
RH	relative humidity
R_p	radius of packing particles, assuming uniform spheres
R_v	evaporation rate
R_{vmax}	maximum evaporation rate
Sc	Schmidt number
t	time
T	temperature
V, V_A	average axial interstitial air velocity, approach velocity
W_{bf}, W_{eq}, W_{crit}	water content of biofilm, at equilibrium with the air phase, when the surface free water phase just disappears
x	coordinate for depth in biofilm, perpendicular to biofilm surface
X, X_{act}, X_{inact}	total biomass concentration in biofilm, active, inactive
Y	yield coefficient
z	axial coordinate in the reactor

Greek letters

β	inactive biomass formation constant
β_1, β_2, β_3	functions describing effects of temperature, water, and air-phase concentration on elimination capacity
Φ	evaporation rate function
μ, μ_i, μ_{max}, μ_{imax}	Monod biomass growth rate constants: general, for species i, maximum, maximum for species i
μ_w	viscosity of water
ν_R, ν_C	stoichiometric coefficient for reactant and contaminant in biodegradation
θ	porosity of reactor packing
ρ_w	density of water

and investigator-by-investigator basis would be impossibly long, and because many models contain common elements, it would be highly repetitive. We have instead chosen to organize the review in terms of the phenomena being modeled and how they have been dealt with.

2. Biofilter and biotrickling filter mechanics

Among modelers there is general agreement on the mechanisms of biofilters and biotrickling filters (Fig. 1). Contaminants are carried into the biofilter by the air at such rates that the flow is presumed to be laminar, although dispersion occurs because of the tortuosity of the pores in the porous packing. As the air passes through the packing, contaminants are transferred from the air to the water in the biofilm. The contami-

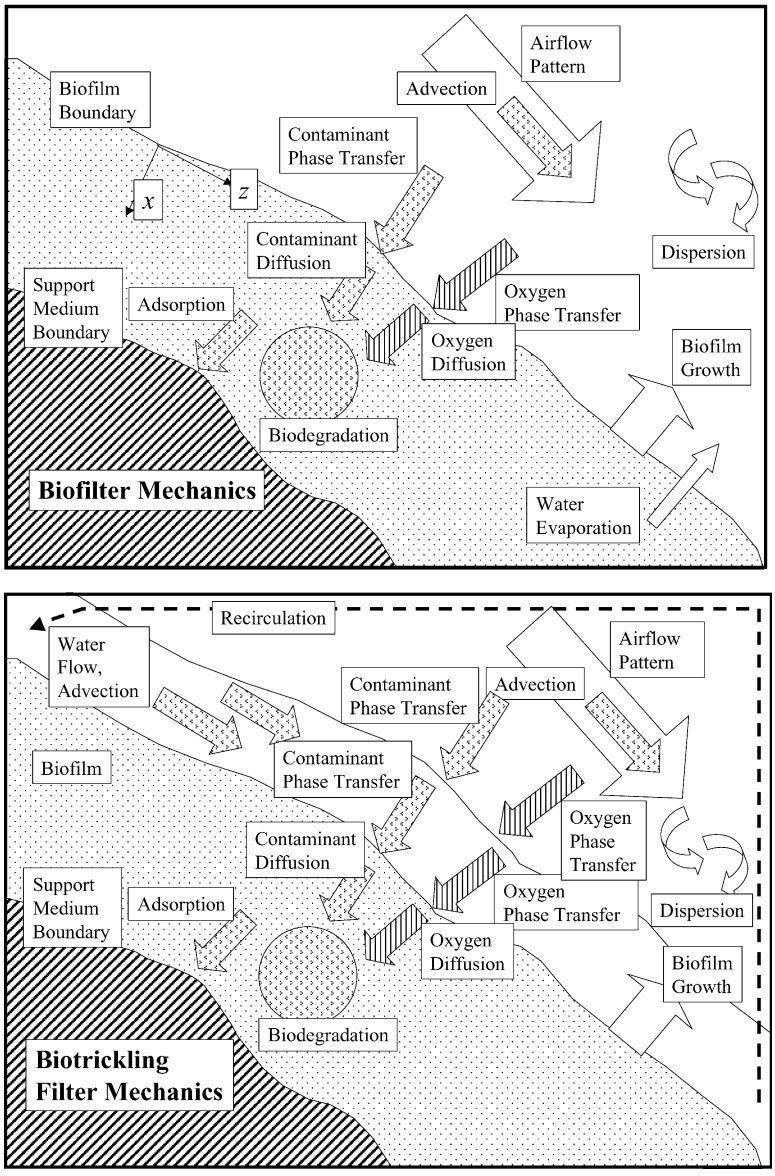

Fig. 1. Phenomena involved in the operation of biofilters and biotrickling filters.

nants diffuse into the depths of the biofilm, and microorganisms in the biofilm absorb the contaminants and biodegrade them. Contaminants may also be adsorbed at the surface of the packing. The great majority of reactors utilize aerobic respiration, so that oxygen and nutrients must also dissolve in the water or biofilm and diffuse to the microorganisms. During operation at moderate-to-high concentrations of contaminant, the biofilm will gradually grow thicker. At some point, diffusion will no longer provide all the needed compounds to the deeper portions of the biofilm, and they will become inactive. Because the pores within the packing are highly irregular in shape, the growing biofilm will change the pore size distribution.

The moving layer of water in biotrickling filters provides operators with a greater degree of control. It ensures a high water content in the biofilm. It is generally recirculated from a storage tank, where pH and nutrient concentration can be monitored and controlled. It may also encourage some sloughing of biofilm, reducing clogging. Some modelers have presumed that the water layer in biotrickling filters represents a negligible barrier to contaminant transfer, and so have ignored it. Others have included the layer of moving water explicitly. Typically, the layer is presumed to be well mixed because of its rapid flow. Mass transfer occurs from the air, and again at the interface between the water layer and the biofilm [1]. Other phenomena, however, may be significant: the water carries contaminant downward (which may be either co-current or counter-current to air flow) and if the water is recirculated, any contaminant remaining in the water as it exits the bottom of the biofilter may be returned to the system at the top. In a system in which the air is flowing upwards, contaminant may be transferred from the recirculating water

to the outgoing air, causing some reduction in removal efficiency. The thickness of the flowing water layer has been approximated by Alonso et al. [2] as:

$$L_{\mathrm{bf}} = \left(\frac{Q_{\mathrm{w}} 3 \mu_{\mathrm{w}}}{a_0 H_{\mathrm{T}} \rho_{\mathrm{w}} g} \right)^{1/3} \tag{1}$$

where Q_{w} is the water flow rate, μ_{w} the viscosity, a_0 the surface area of the packing, H_{T} the height of the tower, ρ_{w} the density, and g is the acceleration of gravity.

It is commonly observed, however, that in biotrickling filters the flowing water does not produce a uniform layer, but wets some of the packing surface while leaving other parts exposed to the gas phase. Kim and Deshusses [3] modeled this effect, using a previously developed empirical relationship to predict the fraction of packing surface wetted.

3. Air flow

3.1. Advective transport in plug flow

Most biofilter or biotrickling filter models assume that air flow within the reactor can be adequately modeled as "plug flow". Under these conditions, the effects of advection can be modeled in one dimension as:

$$\left[\frac{\mathrm{d}C_{\mathrm{air}}}{\mathrm{d}t} \right]_{\mathrm{adv}} = -V \frac{\partial C_{\mathrm{air}}}{\partial z} \tag{2}$$

where t is time, C_{air} the concentration of the contaminant in the air, V the interstitial flow velocity, and z is the axial dimension of the biofilter. Interstitial flow rates are higher than approach velocities:

$$V = \frac{V_{\mathrm{A}}}{\theta} \tag{3}$$

where V_{A} is the approach velocity and θ is the porosity of the medium. Flow in the non-axial dimensions is commonly considered negligible—models are typically one-dimensional.

3.2. Longitudinal dispersion

Because there are typically no radial gradients in concentration, radial dispersion has no effect and is neglected. Axial gradients may be substantial, however so, a few models have considered the possibility of axial dispersion. Hodge and Devinny [4] produced such a model that modeled dispersion in the form:

$$\left[\frac{\mathrm{d}C_{\mathrm{air}}}{\mathrm{d}z} \right]_{\mathrm{disp}} = D_{\mathrm{flow}} \frac{\partial^2 C_{\mathrm{air}}}{\partial z^2} \tag{4}$$

where D_{flow} is the dispersion coefficient. However, both calculations and experiment indicated that axial dispersion was negligible except for biofilters operating at high flow rates—with empty bed detention times of a few seconds [5]. While dispersion occurs as a result of molecular diffusion, in biofilters and biotrickling filters the dominant process is dispersion resulting from the tortuosity of flow.

3.3. Detailed models of air flow

Only a few models have attempted to depict the flow field in greater detail, including pore-level variations in flow speed and direction. Nukunya et al. [6] produced a pore-network biofilter model in which the pore space was modeled as a cubic lattice of tubes, with various tube diameters chosen according to a realistic pore size distribution and placed randomly within the lattice. At each step in the calculation, the air flow field was recalculated to reflect the effects of the decrease in pore diameters as the biofilm grew. Flows perpendicular to the biofilter axis varied on a tube-by-tube basis and possible wall effects were implicitly included because the network was of limited extent.

Ozis et al. [7] used a model based on percolation theory that specified the statistical characteristics of packing porosity without specifying a geometry. However, it implicitly recognized that some portions of the pore network in the biofilter could be blocked, producing reduced and irregular air flow.

4. Phase transfer

Transfer of a contaminant from a gas to a stagnant liquid or a biofilm can be viewed as limited by diffusion resistance within a laminar layer of gas near the interface and by resistance within the liquid or biofilm. Water within the biofilm is presumed to be stagnant, so that molecular diffusion is the only transport mechanism. It has been generally accepted that phase transfer is limited by diffusion in the water phase: the pores are relatively small, dispersion caused by advection tends to mix the gas phase, and molecular diffusion constants in water are on the order of 10^4 times lower than those in air (concentrations, and therefore concentration gradients, are generally higher in the biofilm, but usually only by one order of magnitude). Typically, modelers presume that the concentration at the surface of the biofilm is determined by Henry's Law equilibrium with the concentration of contaminant in the bulk air phase, and that the flux of contaminant into the biofilm is controlled by diffusion resistance in the biofilm at the surface:

$$J_{\mathrm{bf}} = D_{\mathrm{w}} \left[\frac{\partial C_{\mathrm{bf}}}{\partial x} \right]_{x=0} \tag{5}$$

where J_{bf} is the flux of contaminant per unit of surface area, C_{bf} the concentration of contaminant in the biofilm, and x is the coordinate perpendicular to the biofilm surface, which is zero at the air–biofilm interface. In a biotrickling filter, it is typical that transfer in the flowing water layer is slower than transport in the air and faster than in the biofilm. The same formulation is used for transfer from water to the biofilm, and a parallel form is used for transfer from the air to the water.

However, some investigators have observed mass transfer resistance at the interface. This is most likely to occur where contaminant solubility is high and biodegradation is rapid. It is less likely in a biofilter treating volatile organic compounds, but Kim and Deshusses [3] observed strong external mass transfer limitation in laboratory and full-scale biotrickling filters treating hydrogen sulfide. In such cases, models presume that transfer is limited by diffusion resistance in a laminar layer of gas at the surface, and transfer occurs at a rate determined by the degree to which the gas–liquid interface of the biofilm is below saturation:

$$J_{bf} = k_{air-bf}\left[\frac{C_{air}}{H} - C_{bf}\right]$$

where k_{air-bf} is the gas transfer coefficient and H is the Henry's Law constant for the contaminant. Li et al. [8] further approximated the gas transfer coefficient for spherical packing particles as:

$$k_{air-bf} = \frac{D_{air}}{2R_p}[2 + 1.1Re^{0.6}Sc^{0.33}]$$

where D_{air} is the gas-phase diffusion constant, R_p the particle radius, Re the Reynolds number, and Sc is the Schmidt number.

Either of the flux terms must be multiplied by the surface area of the biofilm to determine total flux, and divided by the volume of the phase in order to determine changes in concentrations.

5. Diffusion within the biofilm

Diffusion of the contaminant into the biofilm is presumed to follow Fick's Law:

$$\left[\frac{\partial C_{bf}}{\partial t}\right]_{diff} = D_{bf}\frac{\partial^2 C_{bf}}{\partial x^2} \quad (6)$$

where D_w is the molecular diffusion constant of the contaminant in water. While there is general agreement on this form of the equation, there is less certainty about the appropriate values for the diffusion constant. Molecular diffusion constants have been measured in pure water for most compounds, but diffusion within biofilms may be different. The abundance of cells and exuded polysaccharides reduces the cross-section of water actually available for diffusion and restricts the contaminant to diffusion along tortuous pathways. Some investigators have used the empirical equation developed by Fan et al. [9] that relates the diffusion coefficient in the biofilm to the diffusion coefficient measured in water and the total biomass density in the film (in g/L):

$$D_{bf} = D_w\left[1 - \frac{0.43X^{0.92}}{11.19 + 0.27X^{0.99}}\right] \quad (7)$$

Miller and Allen [10] noted that additional complications are possible. In biofiltration of α-pinene, they showed that biological materials in the biofilm would adsorb the contaminant, causing an initial delay in transport but not affecting the steady-state rates of transport. They also found that in biological films, but not in abiotic films, enzymatic reactions rapidly convert α-pinene to a secondary product that is far more soluble, greatly increasing the effective solubility and degradation rates over those predicted for the parent compound.

6. Adsorption on the solid phase

Contaminants that diffuse to the bottom of the biofilm, particularly during the early stages of treatment when the biofilm is thin, may be adsorbed on the surface of the packing. Adsorption capacities vary widely with packing material. For biofilters using activated carbon packing, for example, modeling adsorption is necessary for accurate description of treatment of waste streams in which the concentration varies with time. Some modelers have also assumed that the particles are porous and contain significant amounts of water that can absorb contaminant [11–13]. For biofilters using lava rock, at the other extreme, adsorption of contaminant is negligible. For all of the packing materials, biofilm exopolysaccharides and other biofilm compounds may compete for adsorption sites, reducing adsorption of the contaminant. Finally, adsorption has no effect on steady-state conditions: the adsorbed material is simply an inactive reservoir that has no influence on treatment efficiency.

Adsorption and desorption have been included in non-steady-state models, where it is generally presumed that the mass of material adsorbed per unit surface area at equilibrium is linearly proportional the concentration of the contaminant in the biomass at the bottom of the biofilm, C_{bfbot}.

$$C_{adseq} = K_{ads}C_{bfbot}$$

where K_{ads} is an empirically determined constant. Ranasinghe et al. [14] took this approach but further modeled the adsorption constant as having Arrhenius-type dependence on temperature:

$$K_{ads} = K_0\ \exp\left[\frac{-\Delta H}{RT}\right] \quad (8)$$

where ΔH is the heat of adsorption, R the gas constant, T the temperature, and K_0 is a constant.

Zarook et al. [12] and Ranasinghe et al. [14] also considered non-equilibrium adsorption, assuming the flux from the biofilm to the surface occurred at a rate proportional to the degree to which it was below equilibrium. Their formulations were equivalent to:

$$J_{ads} = k_{ads}(C_{adseq} - C_{ads})$$

where J_{ads} is the flux per unit surface area, k_{ads} the rate constant, and C_{ads} is the concentration adsorbed.

7. Biomass growth and biodegradation

7.1. Monod equation

Biodegradation rates are a fundamental controlling factor for the effectiveness of biofilters. Most commonly, Monod kinetics are assumed for growth as a function of existing concentrations of biomass and the concentrations of contaminant:

$$\frac{dX_{act}}{dt} = \mu X_{act}, \quad \mu = \frac{\mu_{max} C_{bf}}{K_S + C_{bf}}, \quad \frac{dX_{act}}{dt} = Y\frac{dC_{bf}}{dt} \tag{9}$$

where X_{act} is the biomass density, μ the growth constant, μ_{max} the maximum value of the growth constant, K_S the Monod or half-saturation constant, and Y is the biomass yield. For high values of C, the growth rate is constant, and some modelers have presumed that growth follows zero-order kinetics. For low values of C, growth is linear with contaminant concentration, and some modelers have presumed first-order kinetics. However, when the model includes sufficient detail to show biodegradation rates as a function of depth within the biofilm, concentrations will range from the Henry's equilibrium value at the surface of the biofilm to zero at the maximum depth of penetration, so it is likely that both regimes will be encountered and the full form of the Monod equation will be needed. Often the appropriate values for K_S and μ_{max} are uncertain. Both values are strongly dependent on the conditions under which they are determined and most data in the literature are from experiments performed on microorganisms in stirred, well-aerated suspensions, rather than in biofilms (and are highly variable even so). Thus, these parameters are often fitted to the biofilter data developed in the experiment being modeled.

7.2. Oxygen and nutrient limitation

Because the solubility of oxygen in water is low – often much lower than the solubility of the contaminant – it is sometimes determined that oxygen concentrations, rather than contaminant concentrations, will limit the rate of biodegradation. Nutrients, especially for systems using inert media, can be limiting if the amounts supplied by operators are not adequate. Shareefdeen et al. [15] from work by Williamson and McCarty [16,17] have provided criteria that are appropriate for determining when such limitation occurs. First, the ratio of the diffusive power (concentration × diffusion constant) for the secondary compound (R, oxygen or a nutrient) to the contaminant must be smaller than the ratio of stoichiometric requirements for the reaction. Second, the ratio of concentrations must be smaller than the ratio of Monod constants, so that rapid degradation of the more abundant compound does not change the limitation.

$$\frac{C_{Rbf} D_R}{C_{bf} D_{bf}} < \frac{\nu_R M_R}{\nu_C M_C} \quad \text{and} \quad \frac{C_{Rbf}}{C_{bf}} < \frac{K_{SR}}{K_S} \tag{10}$$

where D represents diffusion constants, ν represents stoichiometric coefficients, and R represents molecular weights.

Where oxygen, for example, is determined to be the limiting compound, the Monod rate constant can be defined as [15,18]:

$$\mu = \frac{\mu_{max} C_{O_2 bf}}{K_{SO_2} + C_{O_2 bf}} \tag{11}$$

where $C_{O_2 bf}$ is the concentration of oxygen in the biofilm and K_{SO_2} is the Monod half-saturation constant for oxygen.

In some regimes, two species may be simultaneously limiting (or limiting at different times and places within a single simulation). Alonso and Suidan [19] have used a double-limit Monod formulation, where N is the nitrate concentration:

$$\mu = \left[\frac{\mu_{max} C_{bf}}{K_S + C_{bf}}\right]\left[\frac{\mu_{max} C_{Nbf}}{K_{SN} + C_{Nbf}}\right] \tag{12}$$

where C_{Nbf} is the concentration of nutrient in the biofilm.

Zarook et al. [12] used Haldane kinetics to describe the effects of inhibition by high concentrations of substrate:

$$\mu = \left[\frac{\mu_{max} C_{bf}}{K_S + C_{bf} + \frac{C_{bf}^2}{K_{inh}}}\right]\left[\frac{C_{O_2 bf}}{K_{O_2} + C_{O_2 bf}}\right]$$

where K_{inh} is the Haldane constant for inhibition of degradation of species i in the presence of species j.

In applications, it is frequent that biofilters are used to treat mixed effluents, and it is possible that they will interact. Deshusses et al. [13] tested three models of interaction and decided that for methyl isobutyl ketone and methyl ethyl ketone, the best was a modified Michaelis–Menton equation equivalent to the Monod form:

$$\mu_i = \left[\frac{\mu_{i\,max} C_{ibf}}{K_{Si} + C_{ibf} + p_{ij} C_{jbf}}\right]$$

where the subscripts i and j refer to two contaminants being treated simultaneously, and p_{ij} is the inhibition constant.

Nguyen et al. [20] have described the inhibition among various contaminants in general using inhibition constants, p_{ij}, for each pair of contaminants, and including oxygen limitation:

$$\mu_i = \left[\frac{\mu_{i\,max} C_{ibf}}{K_{Si} + \sum p_{ij} C_{jbf}}\right]\left[\frac{C_{O_2 bf}}{K_{SO_2} + C_{O_2 bf}}\right]$$

where $p_{ii} = 1$.

In some cases, factors other than nutrient availability may limit biofilm activity. In particular, temperatures may be too low or too high, and the biofilm water content may be too low. Morales et al. [21] made experimental determinations of biofilter performance over a range of temperature and water content conditions and proposed an empirical formula for overall performance:

$$\text{elimination capacity} = EC_{max}\beta_1(T)\beta_2(W_{bf})\beta_3(C_{air}) \tag{13}$$

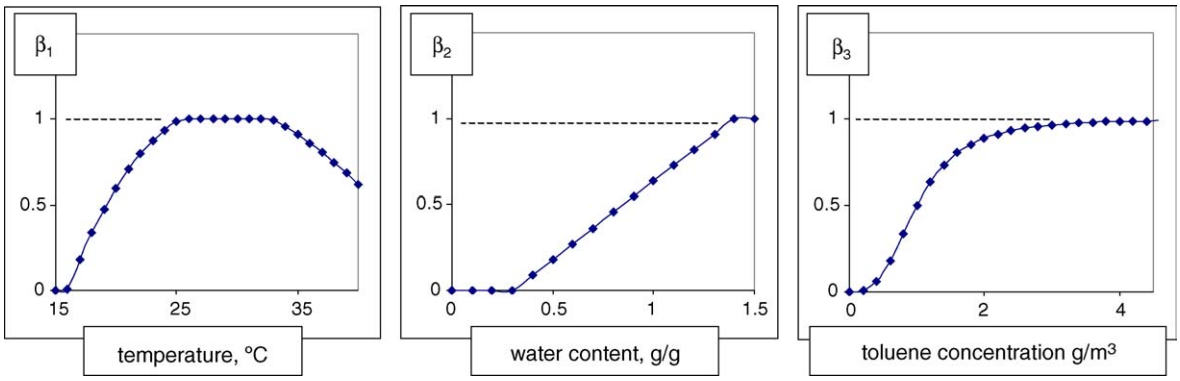

Fig. 2. Effects of temperature water content and gas-phase concentration on biofilter performance. Vertical axes are values of β_i.

where T is the temperature, W the water content, C_{air} the gas-phase contaminant concentration, and β_1, β_2, and β_3 are functions fitted to the data (Fig. 2).

Thus, activity rises with temperature to an optimum range between about 25 and 33 °C, and rises linearly with water content above a critical value until it reaches an optimum. While the formula applies to overall biofilter performance rather than a point within the biofilm, the effects of contaminant concentration have a form much like Monod kinetics.

Okkerse et al. [22] also included a biodegradation rate multiplier that indicated the effects of pH:

$$F_{pH} = \exp\left[-A(pH - B)^2\right] \tag{14}$$

where B is the pH of maximum activity and A is a constant that is inversely proportional to the range of pH over which the organisms can be active.

In most models, it is presumed that reactor operators control nutrient concentrations, and the purpose of modeling the effects of nutrients is simply to determine what supply rates are appropriate. In a few cases, the effects of nutrient regeneration during the oxidation of dead biomass have been included with consumption [23]. In such cases, nutrients are presumed to be released at a rate proportional to biomass degradation, with the constant of proportionality representing the nutrient content of the biomass.

Where oxygen limitation is assumed, it is necessary to know the oxygen concentration profile within the biofilm. In these cases, oxygen concentrations are calculated just as contaminant concentrations are: equilibrium with the gas phase is presumed at the surface, and concentrations within the biofilm are controlled by diffusion through the film and by consumption in biodegradation.

Okkerse et al. [22] modeled a system degrading dichloromethane and producing hydrochloric acid. They assumed that pH also controls biodegradation rates and, in turn, pH is controlled by biogeneration of acids and the buffering capacity of the biofilm. Acid production was proportional to biodegradation rates and buffer concentrations were controlled by diffusion and equilibrium chemistry.

8. Biofilm growth

Biomass growth produces a corresponding thickening of the biofilm. This thickening means that deeper portions of the biofilm receive less contaminant and oxygen, and become less efficient. In one case, it was shown that biofilm farther than 75–100 μm from the surface was no longer active [7]. The thickening biofilm reduces pore sizes, and beginning with the smallest pores, plugs them. The surface area available for mass transfer from the air phase declines. Pressure drops will increase. Thus, long-term biofilter models must recognize the phenomenon of biofilm growth. Biofilm growth is frequently ignored in modeling for moderate or short duration, as this is adequate for understanding phenomena not related to clogging, and greatly simplifies the models.

Growth of the biofilm as a whole is equal to net growth of the film throughout its depth:

$$\frac{dX_{act}}{dt} = \int_0^{L_{bf}} \left(\frac{Y\mu_{max}C_{bf}}{K_S + C_{bf}} - b + \beta b\right) X_{act}\, dx \tag{15}$$

where b is the death rate constant (presuming that death rates are proportional to the amount of biomass present) and β is the inactive biomass accumulation constant (assuming a constant fraction of dying biomass is preserved as inactive material. Song and Kinney [24] approximated this integral by dividing the biofilm into layers and treating each layer as a cell in a cellular automaton model. Biomass grew in each cell according to Monod kinetics, died at a rate proportional to the amount of biomass present, and contributed a constant fraction of the dying cells to the store of dead biomass. When the total biomass present exceeded a preset value, the excess was pushed into the next outward cell.

Okkerse et al. [22] assumed that the biomass death rate was also dependent on oxygen concentration with a Monod-type relationship:

$$b = k_d \frac{C_{O_2bf}}{K_{Sd} + C_{O_2bf}} \tag{16}$$

where k_d and K_{Sd} are constants.

8.1. Evaporation

Sufficient water content is necessary for biofilm activity, and failures of biofilters have frequently been ascribed to the difficulty of keeping water content high and uniform within the packing material. Water is removed by evaporation if the incoming air is at relative humidities less than 100%, or if the metabolic activity of the biofilm releases heat that raises the temperature of the air as it passes through the packing. The dynamics of evaporation have been little studied, but Morales et al. [21] created a model for predicting local evaporation rates. They found that the instantaneous evaporation rate, R_v, could be described as an empirical function of the maximum rate, $R_{v\max}$:

$$R_v = \varphi R_{v\max} \tag{17}$$

where the maximum rate depends on air velocity, V, temperature, T, and relative humidity, RH, and the fitted constants a, c, and d:

$$R_{v\max} = aV^c T^d[\ln(\mathrm{RH})] \tag{18}$$

and φ is a function of the degree to which the biofilm water content, W_{bf}, exceeds the water content, W_{eq}, that would be in equilibrium with the gas phase and on the critical water content, W_{crit}, at which a surface free water phase just disappears:

$$\varphi = f\left(\frac{W_{bf} - W_{eq}}{W_{crit} - W_{eq}}\right) \tag{19}$$

Mysliwiec et al. [23] created an elaborate model for heat and mass transport in biofilters that included evaporation of water and its movement in unsaturated flow. Heat was modeled with terms for air and water advection, conduction of heat through the biofilter packing, water evaporation, and biological production. The liquid water content of the packing changed in response to gravitational water flow, water movement by unsaturated flow, biological water generation, transfer of water from the biofilm to the water phase, and evaporation. Toluene gas-phase concentrations were controlled by advection, dispersion, transfer to the liquid phase, and changes in the volumes of the gas and liquid phase. The model included the effects of nitrogen as a limiting nutrient, and how the concentrations were affected by advection and dispersion in the liquid phase, biological consumption, transfer from the water to the biofilm, release of nutrient by biomass decay, and nutrient additions.

Ranasinghe et al. [14] developed another model for water and energy dynamics within a biofilter. It presumed that the water content of the air was in equilibrium with that in the biofilm, but determined the amount of evaporation necessary to maintain that equilibrium from an energy balance equation. The change in heat content reflected in changes in biofilter temperature was assumed to result from heat carried by advection of warm air, the latent heat of water evaporation, the heat transport by water moving by unsaturated flow, conduction of heat in the biofilter packing, and heat produced by biological activity. When all of these factors were accounted for, evaporation rates and the water content of the biofilter packing could be predicted.

Both the Mysliwiec et al. [23] and Ranasinghe et al. [14] models predicted that biofilters operated without vigorous water input would be subject to drying, as is often seen in practical experience.

9. Surface morphology of the packing and biofilm

9.1. The flat plate model

Some of the most difficult aspects of biofilter modeling are associated with the shape of the biofilm. Early models considered the biofilm a flat layer of uniform thickness, with a surface area equal to the surface area of the porous packing. Real biofilter biofilms are quite different. At the smallest scale, they have a complex shape resulting from their internal dynamics. Picioreanu et al. [25] developed three-dimensional models of biofilms in water showing that initial irregularities are magnified because protuberances reach into regions of higher contaminant concentration, grow faster and become ever more protuberant. A biofilm of closely spaced "fingers" developed, looking much like the morphology seen in scanning confocal microscope photographs of biofilms. However, they also showed that contaminant concentrations in the spaces between the fingers tend to be depleted, so that most activity is confined to the fingertips, and this may mean that the flat layer approximation is still appropriate.

Even if the biofilm can be approximated as a uniform layer, however, the packing particles have rough surfaces, the pores formed between the particles of the packing are highly irregular in shape, and the pores occur in a huge range of sizes. Biofilm growing in the corners and crevices has less access to the air flow than biofilm growing on the surface of a large pore. The smallest pores of the packing will fill rapidly with biofilm, excluding the air. Because the numerous small pores account for a substantial fraction of the surface area, this clogging immediately begins to reduce the surface area available for mass transfer and the volume of near-surface biofilm, even long before clogging becomes noticeable through its effect on head loss.

All models attempting to deal with realistic biofilm conformations are hampered by the difficulty of obtaining data describing the surface of the packing. The size distribution of the packing grains may be known, and there are existing methods such as mercury porosimetry that can measure pore size distribution, but it is difficult to translate this to a description of the shapes and connectivity of the pores. While most models assume spherical particles, most packing materials are strongly non-spherical. Further, the biofilm does not grow in a uniform layer. Thus, progress in this area awaits better tools for characterizing the conformation of the pores and the biofilm surface.

9.2. Irregular biofilm growth

Baltzis et al. [26] observed that biofilms often grow irregularly on the packing material, in "patches" of biofilm that formed as colonies developed around cells from the inoculum and grew laterally. They created a model that assumed differing patches of biofilm devoted to degradation of different compounds in the contaminant mixture. Within each patch, the biofilm was presumed uniform.

Schwarz et al. [27] and Nukunya et al. [28] explicitly considered the changes in air flow regime caused by accumulating biomass, and in turn, the effects of the altered flow on biofilm growth. They imagined a cubic lattice of pores, and chose pore diameters randomly from an assumed pore size distribution. A typical biofilm model, assuming Monod kinetics, was used to determine how the biofilm grew in each pore. Consumption of the contaminant by the biofilm in each pore was used to determine how much the concentration was reduced as the air passed through the pore, and the outputs from each pore were presumed to mix completely at the pore intersections, determining the input concentrations for the subsequent pores. At each time iteration, the new pore diameters (reduced by biofilm growth) were used to calculate a new air flow field for the entire network. Pores that were clogged (the remaining diameter became so small that air flows were negligible) were removed from the calculation, so the model included the effects of local clogging and isolation of some regions surrounded by clogged pores. However, the pores were modeled as cylinders to provide needed simplification for the calculation.

While both of these approaches reflect the observation that biofilm growth rates may be different in different pores, they still assume biofilm uniformity within a pore or patch.

9.3. Packing surface and biofilm morphology

Alonso et al. [2] developed a model in which biofilm grew at a constant rate on the surface of packing that was presumed to consist of regularly packed spheres of equal size. At the point where the spheres are in contact, the surfaces of the biomass on each sphere were blocked by the biomass growing on the other. As the biofilm grows, these occluded areas increase, recognizing that biofilm in corners and crevices can lose it effectiveness. The area remaining was calculated as a function of the radius of the spheres and the thickness of the biomass:

$$a_{bf} = \frac{a_0}{2}\left(1 + \frac{L_{bf}}{R_p}\right)\left[(2-n)\frac{L_{bf}}{R_p} + 2\right] \quad (20)$$

where a_{bf} is the biofilm surface, a_0 the surface area of the spheres, L_f the thickness of the biofilm, R_p the radius of the spheres, and n is the average number of contacts between spheres. This approach has been adopted by Morgan-Sagastume et al. [29] and Song and Kinney [24].

The growth of the biofilm reduces pore sizes and eventually fills some. Additionally, some pores may be filled with biomass, making them useless for treatment. Others may remain unfilled but be surrounded by filled pores, again isolating them from the air phase. Shariati et al. [30] and Ozis et al. [18] developed a model utilizing the principles of percolation theory. In this approach, which has been applied to flow of oil in subsurface reservoirs, the domain is presumed to consist of pores with connecting pathways. No specific geometry was presumed, but the pore size distribution and average connectivity between the pores were utilized. As some pathways closed, flow was restricted, and as closed pathways become numerous, the probability rose that volumes within the domain will be isolated by the closure of surrounding pores. In the biofilter model, an initial pore size distribution is determined [18] or assumed. As the biofilm thickness increases, all of the pores are reduced in size. The pores of radius smaller than the thickness of the biofilm are clogged, and functions dependent on the connectivity of the distribution and functions developed from computer simulations are used to estimate the number of pores surrounded by clogged pores.

In these simulations, removal efficiency initially grows rapidly as the biofilm thickens and more active biomass becomes available. Relatively quickly, however, the film reaches the thickness equal to the deepest penetration of the contaminant (or the needed oxygen). After this, further thickening of the biofilm produces no further improvements in contaminant removal because microorganisms are dying as fast as they are growing, and the net effect is just to add inactive biofilm beneath a surface active layer. From this point on, removal efficiency declines as the pores grow smaller and the smallest pores are plugged, until near the end when the number of isolated pores grows suddenly and the biofilter clogs.

10. The current state of modeling and future challenges

Current models for mass movement in the air and within simple biofilms seem adequate. The major remaining uncertainty is in determination of appropriate diffusion constants for various contaminants that reflect conditions in biofilms rather than water.

Biodegradation rates and biofilm growth models remain somewhat uncertain because of the lack of knowledge of Monod constants and maximum growth rate constants for actual conditions in biofilters. It has become clear that biofilms are a special and peculiar environment for microorganisms, with conditions much different from those in suspended cultures, where the constants can be easily measured.

We have also learned that even biofilms growing on a flat surface are not masses of uniform thickness and consistency. Instead, recent studies with confocal laser microscopy have shown that biofilms are lumpy and irregular and filled with channels that allow water to flow through. Modeling of the true conformations has only just begun, and currently can

produce results no better than those that assume a flat layer of uniform consistency.

Some significant steps forward have been made in considering the complex geometry of the pores. Investigators still assume a biofilm of constant thickness and consistency, but are beginning to deal with the obvious fact that it must be wrapped around packing grains with various shapes, that it thickens with time, and that pores decrease in size and become blocked.

Overall, biofilter modeling remains primarily a research tool. Published models vary in the phenomena they include and the parameters they utilize and they tend to be applicable primarily to the systems studied by the investigator. It is still common that parameters are fitted to results. Such efforts may demonstrate that we understand the phenomena, but they do not allow us to say what will happen in the next biofilter. The ultimate objective of modelling – a single approach that can fit most cases and accurately predict results in advance – is not yet available. Models are not sufficiently reliable for detailed design of a system being applied to a new effluent. Instead, we use the "rules of thumb" gained through experience or, for greatest reliability, a pilot test.

References

[1] J.W. Barton, X.S. Zhang, B.H. Davison, K.T. Klasson, Predictive mathematical modeling of trickling bed biofilters, in: Proceedings of the USC-TRG Conference on Biofiltration, Los Angeles, CA, October, 1998.

[2] C. Alonso, X. Zhu, M.T. Suidan, B.R. Kim, B.J. Kim, Mathematical model of biofiltration of VOCs: effect of nitrate concentration and backwashing, J. Environ. Eng. 127 (7) (2001) 655–664.

[3] S. Kim, M.A. Deshusses, Development and experimental validation of a conceptual model for biotrickling filtration of H_2S, Environ. Prog. 22 (2) (2003) 119–128.

[4] D.S. Hodge, J.S. Devinny, Modeling removal of air contaminants by biofiltration, J. Environ. Eng. 121 (1) (1995) 21–32.

[5] D.S. Hodge, J.S. Devinny, Determination of biofilter model constants using mini-columns, J. Environ. Eng. 123 (6) (1997) 577–585.

[6] T. Nukunya, J.S. Devinny, T.T. Tsotsis, Application of a pore network model to a biofilter treating ethanol vapor, Chem. Eng. Sci. 60 (3) (2004) 665–675.

[7] F. Ozis, Y. Yortsos, J.S. Devinny, A numerical percolation model for describing biomass clogging in biofilters, in: F.E. Reynolds (Ed.), Proceedings of the 2002 Conference on Biofiltration, The Reynolds Group, Tustin, CA, October 31–November 1, 2002.

[8] H. Li, J.R. Mihelcic, J.C. Crittenden, K.A. Anderson, Field measurements and modeling of two-stage biofilter that treats odorous sulfur air emissions, J. Environ. Eng. 129 (8) (2003) 684–692.

[9] L.S. Fan, R. Leyva-Ramos, K.D. Wisecarver, B.J. Zehner, Diffusion of phenol through a biofilm grown activated carbon particles in a draft-tube three-phase fluidized bed bioreactors, Biotechnol. Bioeng. 35 (1990) 279–286.

[10] M.A. Miller, D.G. Allen, Modelling transport and degradation of hydrophobic pollutants in biofilms in biofilters, in: Proceedings of the USC-TRG Conference on Biofiltration for Air Pollution Control, Los Angeles, CA, October, 2004.

[11] H. Jorio, B. Payre, M. Heitz, Modeling of gas-phase biofilter performance, J. Chem. Technol. Biotechnol. 78 (2003) 834–846.

[12] S.M. Zarook, A.A. Shaikh, Z. Ansar, Development, experimental validation and dynamic analysis of a general transient biofilter model, Chem. Eng. Sci. 52 (5) (1997) 759–773.

[13] M.A. Deshusses, B. Hamer, I.J. Dunn, Behavior of biofilters for waste air biotreatment. 1. Dynamic model development, Environ. Sci. Technol. 29 (1995) 1048–1058.

[14] M.A. Ranasinghe, P.J. Jordan, P.A. Gostomski, Modelling the mass and energy balance in a compost biofilter, in: Proceedings of the A&WMA 95th Annual Meeting and Exhibition, Baltimore, MD, June 18–24, 2002.

[15] Z. Shareefdeen, B.C. Baltzis, Y.S. Oh, R. Bartha, Biofiltration of methanol vapor, Biotechnol. Bioeng. 41 (5) (1993) 512–524.

[16] K.J. Williamson, P.L. McCarty, Model of substrate utilization of bacterial films, J. Water Pollut. Control Federation 77 (1976) 955–962.

[17] K.J. Williamson, P.L. McCarty, Verification studies of the biofilm model for bacterial substrate utilization, J. Water Pollut. Control Federation 48 (1976) 281–296.

[18] F. Ozis, A. Bina, J.S. Devinny, Application of a percolation-biofilm growth model to a biofilter with known packing particle size distribution, in: Proceedings of the 2004 Conference on Biofiltration, J.S. Devinny, Redondo Beach, CA, October 21–23, 2004.

[19] C. Alonso, M.T. Suidan, Dynamic mathematical model for the biodegradation of VOCs in a biofilter: biomass accumulation study, Environ. Sci. Technol. 32 (20) (1998) 3118–3123.

[20] H.D. Nguyen, C. Sato, J. Wu, R.W. Douglass, Modeling biofiltration of gas streams containing BTEX components, J. Environ. Eng. 123 (6) (1997) 615–621.

[21] M. Morales, S. Hernandez, T. Cornabe, S. Revah, R. Auria, Effect of drying on biofilter performance: modeling and experimental approach, Environ. Sci. Technol. 37 (2003) 985–992.

[22] W.J.H. Okkerse, S.P.P. Ottengraf, B. Osinga-Kuipers, M. Okkerse, Biomass accumulation and clogging in biotrickling filters for waste gas treatment. Evaluation of a dynamic model using dichloromethane as a model pollutant, Biotechnol. Bioeng. 63 (40) (1998) 418–430.

[23] M.J. Mysliwiec, J.S. VanderGheynst, M.M. Rashid, E.D. Schroeder, Dynamic volume-averaged model of heat and mass transport within a compost biofilter. I. Model development, Biotechnol. Bioeng. 73 (4) (2000) 283–294.

[24] J. Song, K.A. Kinney, A model to predict long-term performance of vapor-phase bioreactors: a cellular automaton approach, Environ. Sci. Technol. 36 (2002) 2498–2507.

[25] C. Picioreanu, M.C.M. van Loosdrecht, J.J. Heijnen, Mathematical modeling of biofilm structure with a hybrid differential-discrete cellular automaton approach, Biotechnol. Bioeng. 58 (1) (1998) 101–116.

[26] B.C. Baltzis, S.M. Wojdyla, S.M. Zarook, Modeling biofiltration of VOC mixtures under steady-state conditions, J. Environ. Eng. 123 (6) (1997) 599–605.

[27] B.C.E. Schwarz, J.S. Devinny, T.T. Tsotsis, A biofilter network model—importance of the pore structure and other large-scale heterogeneities, Chem. Eng. Sci. 56 (2001) 475–483.

[28] T. Nukunya, T.T. Tsotsis, J.S. Devinny, Application of a pore network model to a lava rock biofilter treating ethanol, in: F.E. Reynolds (Ed.), Proceedings of the 2002 Conference on Biofiltration (an Air Pollution Control Technology), The Reynolds Group, Tustin, CA, October 31–November 1, 2002.

[29] F. Morgan-Sagastume, B.E. Sleep, D.G. Allen, Effects of biomass growth on gas pressure drop in biofilters, J. Environ. Eng. 127 (5) (2001) 388–396.

[30] M. Shariati, C. Lu, J.S. Devinny, Y. Yortsos, Application of percolation theory to biofilm accumulation and head loss in biofilters, in: F.E. Reynolds (Ed.), Proceedings of the 2000 Conference on Biofiltration (an Air Pollution Control Technology), The Reynolds Group, Tustin, CA, October 19–20, 2000.